Cyclotron resonance of conduction electrons in GaAs at very high magnetic fields

N. Miura and H. Nojiri*
Institute for Solid State Physics, University of Tokyo, Roppongi, Minato-ku, Tokyo 106, Japan

P. Pfeffer and W. Zawadzki
Institute of Physics, Polish Academy of Sciences, 02-668 Warsaw, Poland

(Received 10 February 1997)

Cyclotron resonance of conduction electrons in GaAs was measured at a photon energy of 224 meV in magnetic fields up to 500 T produced by an electromagnetic flux compression. Cyclotron resonance and the corresponding transitions between donor states (magnetodonor transitions) were resolved at fields of about 190 T. The free-electron cyclotron resonance was successfully described by the five-level $\mathbf{P}\cdot\mathbf{p}$ model of band structure, which confirms the validity of the model up to 370 meV above the band edge. It was demonstrated that the spin g value goes through zero and changes sign as a function of magnetic field. Resonant and nonresonant polarons were included in the theory and it was found that the Fröhlich polaron coupling constant $\alpha=0.085$ gives the best fit to the data. The experimental results of the magnetodonor transitions were analyzed and well accounted for by an effective two-level $\mathbf{P}\cdot\mathbf{p}$ model. [S0163-1829(97)07120-8]

I. INTRODUCTION

The structure of the conduction band in GaAs has been investigated for many years.[1–6] Although GaAs is a medium-gap material, its conduction band exhibits pronounced nonparabolicity, which results in the energy dependence of the effective mass and the spin g factor. Experiments at high-magnetic fields have revealed a spin doublet in the cyclotron resonance (CR) of conduction electrons. The doublet is due to energy dependence of the g factor, so that the spin-up and spin-down transitions do not have the same energy. The doublet splitting is observed also for the corresponding transitions between donor states (magnetodonor transitions). It has been shown theoretically[4–6] that the three-level $\mathbf{P}\cdot\mathbf{p}$ model, which is valid for narrow-gap materials InSb and InAs,[7] is not sufficient for GaAs. The reason is that the fundamental gap in GaAs is not really small and, as a result, the interaction of the conduction level with higher conduction levels may not be neglected. Thus, a five-level (5L) model is required.[8]

In our previous work, we studied CR at the laser energy of 130 meV (a magnetic field of about 80 T) and the electron energies involved were around 185 meV.[10] In this work, we study CR spectra for the photon energy of 224 meV at a field of about 190 T. To analyze the very-high-field data we include the $\mathbf{P}\cdot\mathbf{p}$ interaction with far bands (up to the second-order perturbation), which provides an adequate description not only for the conduction band of GaAs, but also for its valence bands.[9] The very-high-field data presented in our paper test the validity of the theoretical 5L model up to the energies of 370 meV above the conduction-band edge (the energy of the upper Landau level), whereas transport experiments and the free-carrier reflection probe the energies not exceeding 200 meV above the edge.[8]

Another interesting aspect of our studies is the behavior of the spin g value. At the band edge of GaAs the Landé factor is very small: $g_0^*=-0.44$. It is predicted theoretically that it should go through zero and change sign as a function of magnetic field. Our experiments show that this is indeed the case.

It has been shown before that one cannot describe the conduction electrons in GaAs without including resonant and nonresonant polaron effects, related to the interaction of electrons with optical phonons.[8,11] Our paper addresses a somewhat controversial issue of the strength of this interaction in GaAs.

High magnetic fields are also of importance in the investigations of donor states since they allow one to reach large values of the parameter $\gamma=\hbar\omega_c/2\ \mathrm{Ry}^*$, which measures the relative strength of magnetic and Coulomb interactions.[12] In our experiments γ has the value of 27.3, never before attained for GaAs.

The present experiments have become possible due to the recent advances in high magnetic-field technology.[13] Our paper begins with a description of the experimental technique using the electromagnetic flux compression, which generates the fields up to 500 T. We then present experimental results on CR in GaAs and their theoretical description. Finally the results of the magnetodonor transitions are discussed.

II. EXPERIMENTS

High magnetic fields were produced by an electromagnetic flux compression.[13–15] As shown in the inset of Fig. 1, we employ a single-turn primary coil and a liner, which are set coaxially. When we supply a large pulse current of the order of 4 MA to the primary coil from a capacitor bank of 4 MJ (40 kV), a secondary current is induced in the liner in the opposite direction and the repulsive force between the two currents rapidly squeezes the liner. By this squeezing motion of the liner we compress the initial magnetic flux and obtain a very high magnetic-flux density when the diameter of the liner becomes sufficiently small. Figure 1 shows typical experimental traces for the primary current and the magnetic field produced by this method. Using a liner with the initial diameter of 150 mm, the thickness of 1.5 mm, and the length

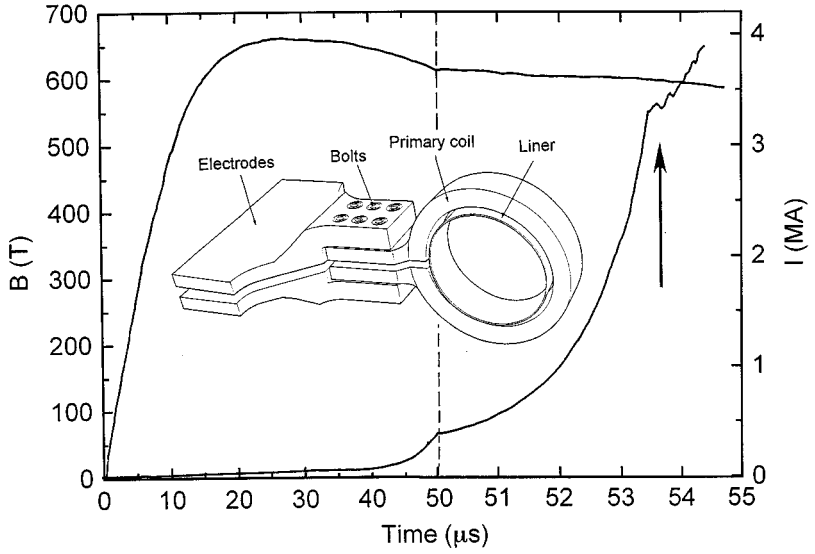

FIG. 1. Wave forms of the primary current and the magnetic field produced by the electromagnetic flux compression method. The time scale is changed at $t=50$ μs to demonstrate the important part with an expanded scale. The inset shows the coil system of the electromagnetic flux compression.

of 55 mm, high magnetic fields up to nearly 500 T are produced reproducibly. Although the rise time is rather short, of the order of several μs, we can obtain clean data of the cyclotron resonance, as shown below.

We employed a CO laser as a radiation source, which produces an infrared radiation at a wavelength 5.527 μm with a power of about 500 mW. To detect the change of the transmission through the sample during the very short pulse field we used a $Hg_xCd_{1-x}Te$ detector, operated at 77 K, together with a fast preamplifier. The signal was transmitted to a recorder through a fiber optics after an electro-optic conversion.

Two GaAs samples were investigated. Sample *A* was grown by molecular-beam epitaxy to a thickness of 2.5 μm, and it had a carrier concentration of 1.0×10^{17} cm^{-3}. Sample *B* was grown by liquid-phase epitaxy, and its thickness, carrier concentration, and mobility were 10 μm, 1.5×10^{16} cm^{-3} and 1.0×10^{5} cm^2/V s at 77 K, respectively. Both samples have a growth direction in the [100] orientation and we applied magnetic field in this direction. The sample temperature was controlled from room temperature down to about 6 K using a disposal flow-type cryostat, and it was measured by a AuFe–Chromel thermocouple. The magnetic field was measured by a pick-up coil wound around the sample.

Figure 2 shows the time dependence of magnetic field during the pulse and the corresponding optical transmission of GaAs (sample A) for the laser wavelength 5.527 μm ($\hbar\omega=224$ meV). Although the rise time of the field is rather short, we can resolve three peaks at the fields of around 190 T. Plotting the transmission at different temperatures as a function of magnetic field we obtain the traces shown in Fig. 3 for the two samples. At higher temperatures one can see three peaks. This is somewhat puzzling since at the lower photon energy of $\hbar\omega=130.5$ meV four peaks were observed.[10] As shown schematically in Fig. 4, the two peaks at higher magnetic fields (corresponding to lower energies at a constant magnetic field) are due to the free electron CR transitions $0^{\pm}\rightarrow1^{\pm}$, whereas the two peaks at lower fields (higher energies) are related to transitions between the associated donor levels: $(000^{\pm})\rightarrow(010^{\pm})$ (in the atomic notation: $1s^{\pm}\rightarrow2p^{\pm}$). At lower temperatures only the donor transitions are usually observed because of the freeze-out effect, at higher temperatures the free-electron transitions are the dominant absorption mechanism.

The traces shown in Fig. 3 exhibit only three peaks (in spite of larger level separations at higher fields), as compared to the data of Ref. 10 due to an accidental coincidence of the free electron CR peak $0^{+}\rightarrow1^{+}$ and the donor peak $(000^{-})\rightarrow(010^{-})$, which are schematically shown in Fig. 4. This conclusion is confirmed by the theoretical analysis presented below.

It should be noted that the spin-down transitions (for both free electrons and donors) have stronger intensity than its spin-up partners. This is because the *g* factor at very high fields is positive for both $n=0$ and $n=1$ Landau levels, as shown in the theoretical section. This means that the 0^{-} state and the corresponding donor state (000^{-}) are the lowest ones.

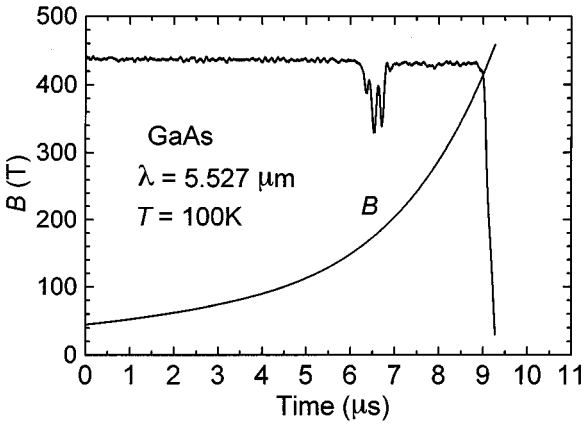

FIG. 2. Time dependence of magnetic field produced by the flux compression (the left scale) and of the optical transmission of GaAs (the right scale, arbitrary units) for sample A.

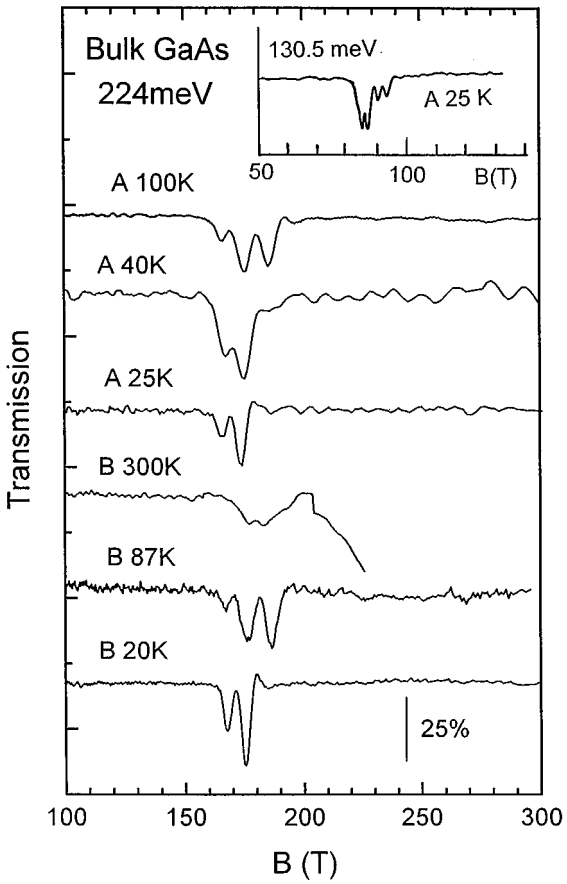

FIG. 3. Transmission traces for two GaAs samples versus magnetic field at the photon energy 224 meV ($\lambda = 9.51\ \mu$m). The temperatures are indicated. Lower field data of Ref. 10 are included as a inset.

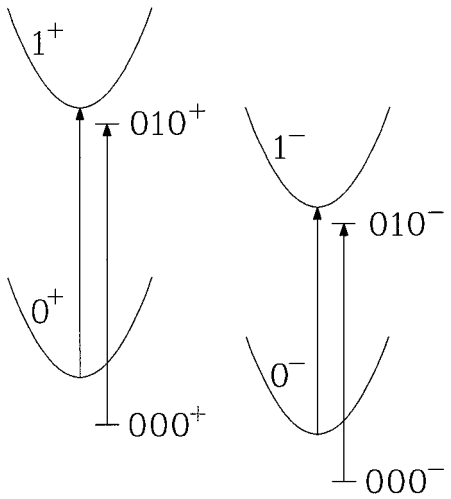

FIG. 4. Cyclotron resonance and impurity-shifted cyclotron resonance transitions for both spin orientations, as observed in GaAs at megagauss fields (schematically).

III. THEORETICAL DESCRIPTION

We describe the conduction band of GaAs using a five-level $\mathbf{P}\cdot\mathbf{p}$ theory and incorporating all other bands within the P^2 approximation.[9] Compared to the ''bare'' five-level model[18] this procedure amounts mainly to adding the valence-band contributions, as described by the Luttinger parameters $\gamma_1, \gamma_2, \gamma_3, \kappa$. The $\mathbf{P}\cdot\mathbf{p}$ theory generalizes the $\mathbf{k}\cdot\mathbf{p}$ scheme for the case of an electron in a periodic crystal potential subjected to an external magnetic field $\mathbf{B}$. One should then replace in the multiband Hamiltonian the wave vector $\hbar\mathbf{k}$ by $\mathbf{P}=\mathbf{p}+e\mathbf{A}$, where $\mathbf{A}$ is the vector potential of the magnetic field. The resulting $\mathbf{P}\cdot\mathbf{p}$ equations for the envelope functions $f_l(\mathbf{r})$ are

$$\sum_l \left[\left(\frac{P^2}{2m_0}+E^{(l)}-E\right)\delta_{l'l}+\frac{\mathbf{p}_{l'l}\cdot\mathbf{P}}{m_0}+\mu_B B\cdot\boldsymbol{\sigma}_{l'l}+H^{\text{s.o.}}_{l'l}\right]f_l = 0, \tag{1}$$

where indices l and l' run over the above bands, m_0 is the free-electron mass, $E^{(l)}$ are the band-edge energies, μ_B is the Bohr magneton, $\boldsymbol{\sigma}$ is the Pauli spin operator, and $H^{\text{s.o}}_{l'l}$ are the interband matrix elements of the spin-orbit interaction. Five levels: $\Gamma_8^c, \Gamma_7^c, \Gamma_6^c, \Gamma_8^v, \Gamma_7^v$, are included explicitly, while far levels are incorporated similarly to the procedure of Kane,[16] Pidgeon, and Brown,[7] and Weiler, Aggarwal, and Lax.[17]

The basis functions for the five levels in question are given in Ref. 8. They diagonalize the spin-orbit interaction within the (Γ_8^c, Γ_7^c) and (Γ_8^v, Γ_7^v) sets. Since the zinc-blende structure does not have inversion symmetry, an off-diagonal matrix element of the spin-orbit interaction between the above sets has to be included, $\Delta^- \sim \langle X^v|[\boldsymbol{\nabla}V, \mathbf{p}]_y|Z^c\rangle$. A value of this term, $\Delta^- = -0.061$ eV, has been determined from pseudopotential calculations by Gorczyca, Pfeffer, and Zawadzki.[18] Three other interband momentum matrix elements appear in the five-level model: $P_0 \sim \langle S|p_x|X^v\rangle$, $P_1 \sim \langle S|p_x|X^c\rangle$, and $Q \sim \langle X^v|p_y|Z^c\rangle$. The elements P_0 and P_1 correspond to mixing of p-type valence-band and higher-lying conduction-band states, respectively, with s-type Γ_6 states, and they are mainly responsible for the band nonparabolicity. The Q matrix element gives rise to anisotropy of the Γ_6 band. In addition, the remote levels influence the Γ_6 band anisotropy by the terms proportional to $\gamma_2 - \gamma_3$. The experimental energy gaps used in the calculations are $E_0 = 1.519$ eV, $E_1 = 2.969$ eV, $\Delta_0 = 0.34$ eV, and $\Delta_1 = 0.171$ eV.[9] The following values of the interband matrix elements are used in the five-level model: $E_{P_0} = 27.8$ eV, $E_{P_1} = 2.361$ eV, and $E_Q = 15.56$ eV (in standard units $E_P = 2P^2/m_0$), the far-band contributions to the effective mass are $F = -1.055$ (corresponding to $C/2$ in Ref. 8), and to the band-edge g value: $N_1 = -0.010\,55$ (corresponding to $C'/2$ Ref. 8). These values result in a conduction-band-edge mass $m_0^* = 0.066 m_0$ (including the nonresonant polaron contribution, see below), and $g_0^* = -0.44$. The far-band contributions to the valence bands, as described by the Luttinger parameters, are $\gamma_1^L = 7.80$, $\gamma_2^L = 2.46$, $\gamma_3^L = 3.30$, $\kappa^L = 2.03$. Quantities γ_i and κ used in the calculations represent modified Luttinger parameters, in which the $\mathbf{k}\cdot\mathbf{p}$ interaction of $vbgb\Gamma_8^v$ level with the $\Gamma_6^c, \Gamma_8^c, \Gamma_7^c$, levels has been subtracted, since it is included explicitly in the matrix. Thus we have

$$\gamma_1=\gamma_1^L-\frac{E_{P_O}}{3E_0}-\frac{E_Q}{3(E_1+E_0)}-\frac{E_Q}{3(E_1+\Delta_1+E_0)},$$

$$\gamma_2=\gamma_2^L-\frac{E_{P_O}}{6E_0}+\frac{E_Q}{6(E_1+E_0)},$$

$$\gamma_3=\gamma_3^L-\frac{E_{P_O}}{6E_0}-\frac{E_Q}{(6E_1+E_0)},$$

$$\kappa=\kappa^L-\frac{E_{P_O}}{6E_0}+\frac{E_Q}{18(E_1+E_0)}+\frac{E_Q}{9(E_1+\Delta_!+E_0)}. \quad (2)$$

The above parameters describe very well all known magnetooptical data at magnetic fields up to 24 T.[9]

One finally deals with 14 coupled differential equations[9] for the envelope functions f_l. Since the conduction band is anisotropic, solutions are found by looking for the envelope functions f_l in the form of sums of harmonic-oscillator functions. An infinite-dimensional matrix is then obtained, in which different Landau states are coupled with Q and γ_l matrix elements. This matrix is subsequently truncated and diagonalized numerically. The direction of magnetic field with respect to the crystal axes is chosen by taking the appropriate gauge. A 35×35 matrix is diagonalized for $\mathbf{B}\|[001]$, and 63×63 matrix for $\mathbf{B}\|[110]$ field directions.

Although GaAs is a weakly polar material and the experiments are performed at energies well beyond the longitudinal-optic-phonon energy ($\hbar\omega_l=36.2$ meV), resonant and nonresonant polaron effects are included in the theoretical description. The nonresonant polaron contribution is important for the $\mathbf{P}\cdot\mathbf{p}$ theory since at $B=0$ the polaron mass is given by[11]

$$\frac{m^*_{\rm pol}}{m^*_0}=\frac{1+\alpha/2}{1+\alpha/3}, \quad (3)$$

where m_0^* is the ''bare'' effective mass. This effect must be accounted for when determining the bare mass from the experimental one, i.e., $m^*_{\rm pol}$. The $\mathbf{P}\cdot\mathbf{p}$ calculation is first performed with the ''bare'' parameters and then the polaron contributions are included to obtain the experimental values. The five-level model is fitted to the low-field data[9] and subsequently extrapolated to high fields.

The widely accepted value of the polar constant for GaAs is $\alpha=0.065$.[19] However, we find that we can obtain an equally good description of the low-field data and a distinctly better description of the megagauss data by taking the value of $\alpha=0.085$, as first suggested by Lindemann *et al.*[19] and discussed by Pfeffer and Zawadzki.[9]

In order to compare the theory with experiment one has to define the observable quantities. The cyclotron mass m^* is defined by relation $E_1^{\pm}-E_0^{\pm}=\hbar eB/m^*=\hbar\omega$, where $E_n^{\pm}$ is the energy of the nth Landau state with the corresponding projection of the spin-angular momentum on the magnetic-field direction. The effective Landé (spin) g factor for the Landau level n is defined by the relation $E_n^+-E_n^-=g_n^*\mu_BB$.

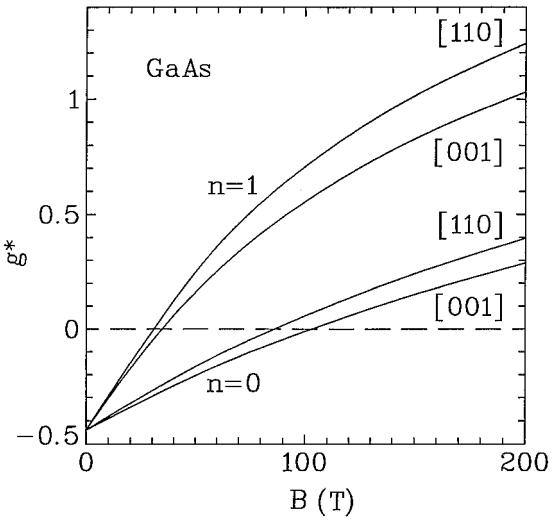

FIG. 5. The Landé factor of conduction electrons in GaAs for the two lowest Landau levels versus magnetic field, as calculated for two field orientations.

IV. RESULTS AND DISCUSSION

The calculated g value for the zeroth and the first Landau level versus magnetic field for two field orientations is shown in Fig. 5. For the experiments at $B\approx80$ T, the g value for the zeroth Landau level is negative and that for the first Landau level is positive.[10] On the other hand, for the experiments at $B\approx190$ T the g value for the initial and final Landau levels is positive. The level scheme for both situations is shown in Figs. 6(a) and 6(b). It can be seen that at $B\approx80$ T the ground state is involved in the transition with higher energy (which occurs at a lower magnetic field for a fixed source energy), while at $B\approx190$ T the ground state is involved in the lower-energy transition (occurring at a higher field for a fixed source energy). This theoretical result is

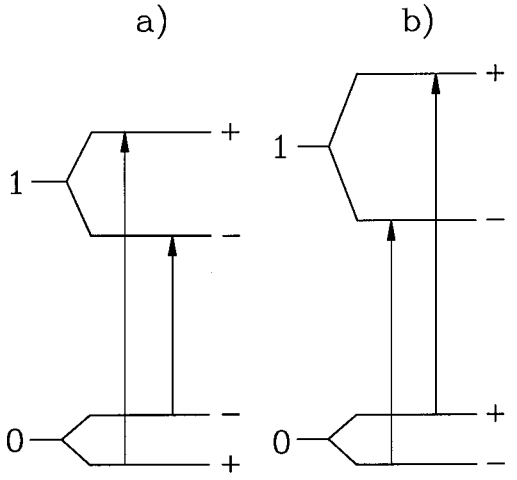

FIG. 6. (a) Schematic diagram of spin-conserving CR transitions in GaAs at $B\approx80$ T. The transition originating from the lowest state has a higher energy than its spin partner. (b) The same as in (a) but for $B\approx190$ T. The transition originating from the lowest state has a lower energy than its spin partner.

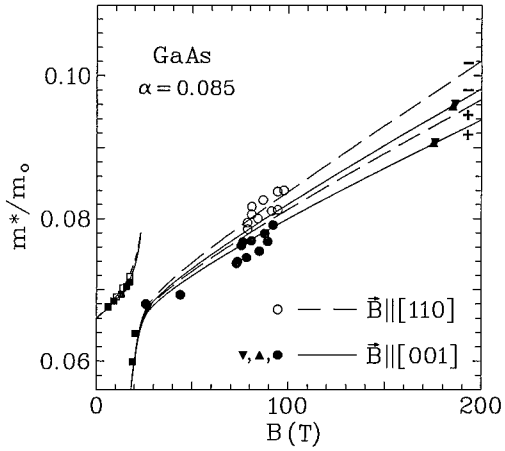

FIG. 7. Experimental and theoretical cyclotron masses of conduction electrons in GaAs (spin-up and spin-down transitions) versus magnetic field for two-field orientations. The points at $B \leqslant 20$ T are after Sigg, Perenboom, and Wyder (Ref. 3) and Hopkins *et al.* (Ref. 5), the points at $B \approx 80$ T are after Najda *et al.* (Ref. 10), those at $B \approx 190$ T are from the data shown in Fig. 3.

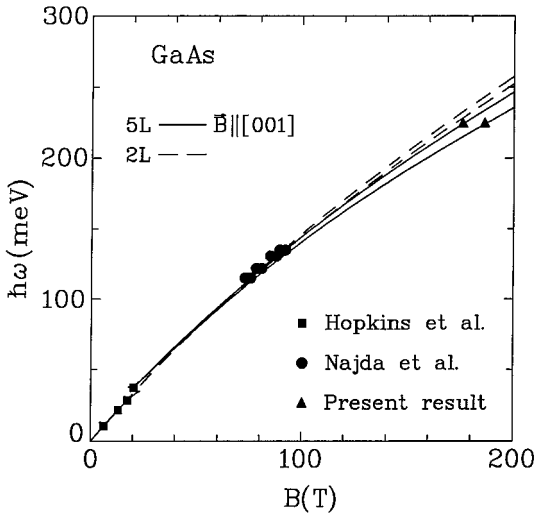

FIG. 8. Cyclotron energies in GaAs versus magnetic field. Dashed lines, two-level model without polaron contributions; solid lines, five-level model with polaron contributions. The experimental data are also indicated.

confirmed by the observed transition intensities at low temperatures: at $B \approx 80$ T the lower field transition is more intense,[10] while at $B \approx 190$ T the higher field transition is more intense. This effect would be more pronounced at still lower temperatures, but it is already visible in our data for both samples (cf. experimental traces for $T = 100$ and 87 K in Fig. 3).

A plot of the cyclotron masses for the two spin directions versus magnetic field is shown in Fig. 7. The discontinuity is due to the resonant polaron effect at fields of about 23 T. The experimental mass anisotropy at $B \approx 80$ T is somewhat higher than that predicted theoretically. On the other hand, the experimental mass value at $B \approx 190$ T agrees very well with the theory. For $B \approx 186$ T we calculate $E_1^- = 367$ meV above the conduction-band edge. The agreement between the experiment and the theory at this field indicates that our description of the conduction band of GaAs is valid at such high energies. At cyclotron energies $\hbar\omega_c \gg \hbar\omega_i$, which is the case in our experiments, one deals with almost bare electron mass (the latter increases at higher fields due to band's nonparabolicity). When the bare band-edge effective mass is calculated using the polar constant $\alpha = 0.065$, the theoretical masses at megagauss fields are somewhat higher than the experimental ones.[9]

The experimental CR energies for $B \| [100]$ are relatively well described by the simple two-level (2L) model of the band structure. This is illustrated in Fig. 8, where the dashed lines are calculated for the experimental band-edge mass $m_0^* = 0.066 m_0$, the Landé factor $g_0^* = -0.44$, and the real energy gap 1.519 eV, using the two-level formula (5) with $\langle V \rangle = 0$ and $\langle K \rangle = 2\gamma(n + \frac{1}{2})$. However, the coincidence of CR energies calculated according to the 2L formula with those given by the full 5L description (including the polaron effects) for $B \| [100]$ is fortuitous. As follows from Fig. 7, for $B \| [110]$ the CR masses are higher than those for $B \| [100]$, which would correspond to lower CR energies for that field direction in Fig. 8. On the other hand, the 2L model gives spherical CR energies. It has been unambiguously demonstrated in experiments on GaAs quantum wells (cf. Zawadzki *et al.*,[20] and the references therein) that the nonparabolicity of the conduction band in GaAs is considerably stronger than that given by the 2L model.

In Fig. 9 we plot the experimental and theoretical differences of resonant magnetic fields for spin-up and spin-down CR transitions (spin-doublet splittings). These differences are directly related to the fact that the g values for $n = 0$ and $n = 1$ Landau levels are different as shown in Fig. 6. It can be seen that the description of the spin-doublet splittings is excellent up to the highest fields, testifying again the validity of the theory at high-electron energies. It should be noted that the spin-doublet splittings obey very well the dependence $\Delta B \sim B^2$ up to the highest fields.[6] We cannot offer any simple explanation of this behavior.

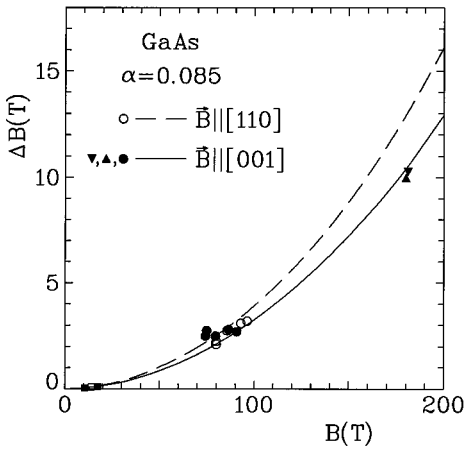

FIG. 9. Experimental and theoretical spin-doublet splittings of the cyclotron resonance in GaAs versus magnetic field for two field orientations. The points at $B \leqslant 20$ T are after Hopkins *et al.* (Ref. 5), the points at $B \approx 80$ T are after Najda *et al.* (Ref. 10), those at $B \approx 190$ T are from the data shown in Fig. 3.

We now turn to the description of the magnetodonor (MD) data. As follows from our analysis of the free-electron properties, the conduction band of GaAs exhibits a pronounced nonparabolicity. This has to be accounted for in the analysis of impurity states. However, there exists at present no MD theory within the framework of the five-level model. Such a calculation would be laborious and would require numerous approximations. There exists a description of MD energies for narrow-gap semiconductors within a three-level model,[21,22] but it is not directly applicable to medium-gap materials. In view of this we treat the problem using an effective two-level model.[22] This is done by fitting the calculated and experimentally confirmed dispersion relation $E(k)$ for the conduction band of GaAs into an effective two-level $\mathbf{k}\cdot\mathbf{p}$ formula,

$$\frac{\hbar^2 k^2}{2m_0^*} = E\left(1+\frac{E}{\varepsilon_g^*}\right), \tag{4}$$

in which the gap takes an adjusted value $\varepsilon_g^* = 0.98$ eV.[8] We want to solve the MD problem variationally. Formula (4) must then be generalized in order to account for the presence of magnetic field and the Coulomb potential. It is convenient to take the symmetric gauge for the vector potential of magnetic field, $\mathbf{A}=[-By/2,+Bx/2,0]$ and to express the energies in the effective Rydbergs, $\mathrm{Ry}^* = m^* e^4/2\kappa^2\hbar^2$, and the lengths in the effective Bohr radii $a_B^* = \kappa\hbar^2/m^* e^2$, where κ is the dielectric constant. The variational MD energies are

$$E_\pm = -\frac{\varepsilon_g^*}{2} + \left\{\left(\frac{\varepsilon_g^*}{2}\right)^2 + \varepsilon_g^*\left(\langle K\rangle \pm \gamma\,\frac{m_0^*}{2m_0}\,(g_0^*-2)\right)\right\}^{1/2} \pm \gamma\,\frac{m_0^*}{m_0} + \langle U\rangle, \tag{5}$$

where

$$K = -\nabla^2 - i\gamma\,\frac{\partial}{\partial\varphi} + \frac{\gamma^2\rho^2}{4}, \tag{6}$$

and

$$\gamma = \frac{\hbar\omega_c}{2\ \mathrm{Ry}^*} = \left(\frac{a^*_B}{L}\right)^2 \tag{7}$$

is the characteristic parameter for the MD problem[23] and $L=(\hbar/eB)^{1/2}$ is the magnetic radius. The brackets $\langle K\rangle$ and $\langle U\rangle$ denote the variational averages of the kinetic energy (6) and the potential energy $U=-2/(\rho^2+z^2)^{1/2}$. Expression (5) follows from Eq. (11) of Ref. 22 in the limit of $E-U \ll \varepsilon_g^* + \frac{2}{3}\Delta$, where Δ is the spin-orbit energy. In addition, the free-electron Pauli term with $g=2$ is explicitly retained (in Ry* units). This term is not negligible in the medium-gap materials, in contrast to the narrow-gap case. It can be easily checked that expanding the square root (in the limit of $K \ll \varepsilon_g^*$) one obtains from Eq. (5) the standard expression for the orbital and spin quantization.

Thus, the calculation of MD energies amounts to separate evaluations of the trial averages $\langle K\rangle$ and $\langle U\rangle$ and a minimization of the energy (5). This is done with the use of atomic-magnetic trial functions, first introduced by Pokatilov and Rusanov[24] and described in some detail by Zawadzki *et al.*[12]

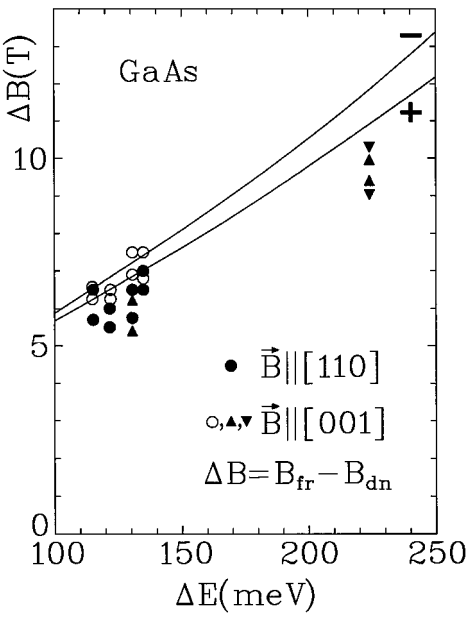

FIG. 10. Experimental and theoretical differences of resonance fields between the donor-shifted and free-electron cyclotron resonances in GaAs (spin-up and spin-down transitions) versus resonance energy. The data around $\Delta E \approx 125$ meV are after Najda *et al.* (Ref. 10). The points at $\Delta E = 224$ meV are from the present work (Fig. 3). The theory neglects band nonsphericity.

The corresponding free-electron energies are calculated within the same model by putting in Eq. (5) the energies $\langle U\rangle = 0$ and $\langle K\rangle = 2\gamma(n+\frac{1}{2})$.

In Fig. 10 we show the observed differences ΔB between the resonance fields for the free-electron and MD-shifted cyclotron resonances, plotted as a function of the resonance (source) energy. The binding energy of the ground MD state (belonging to the zeroth Landau level) is larger than that of the excited state (belonging to the first Landau level), so that the MD-shifted transition has a higher energy. Consequently, for a fixed transition energy the MD-shifted resonance occurs at a lower magnetic field. The solid lines are theoretical, calculated for spin-up and spin-down CR transitions (as illustrated in Fig. 4). Taking into account the uncertainties of the experimental readings and the approximations of the theory, the overall agreement between the two should be considered good. The theory employs the effective two-level model, neglecting thereby the nonsphericity of the band. Experimentally, as can be seen in Fig. 3, the free-electron $0^+ \rightarrow 1^+$ CR transition coincides with the MD-shifted $0^- \rightarrow 1^-$ transition, so that their readings are not precise and they differ somewhat for the two investigated samples. The discrepancy between the experiment and the theory at the highest field is within the uncertainty of the effective Rydberg value 5.8 meV, which does not exceed 10%. The values of transition energies plotted on the abscissa of Fig. 10 indicate explicitly that our experiments reach quite high into the conduction band of GaAs.

V. SUMMARY

Our experiments confirm the theoretical prediction that the g value of conduction electrons in GaAs changes sign

from negative to positive in the megagauss range of magnetic fields. The problem of the electron g value in GaAs going through zero has recently acquired a great significance in relation to the fractional quantum Hall effect[25] and skyrmions.[26] The theory, based on the five-level $\mathbf{P}\cdot\mathbf{p}$ model complemented by far-level contributions, describes well the free-electron properties at energies of up to 370 meV above the band edge, if the polar constant $\alpha=0.085$ is used. The band parameters used in this model also describe quite well the light- and heavy-hole bands of GaAs.[9] An effective two-level $\mathbf{P}\cdot\mathbf{p}$ model successfully accounts for the observed donor shift of the cyclotron resonance at magnetic fields up to 2 MG.

ACKNOWLEDGMENTS

The authors are obliged to Professor H. Sakaki and Dr. H. Noguchi of the University of Tokyo for the gift of the samples (sample A). This work was supported in part by the Polish Committee for Scientific Research under Grant No. 2P03B13911.

*Present address: Institute for Material Research, Tohoku University, Katahira, Sendai, Japan.

[1] J. M. Chamberlain, P. E. Simmons, and R. A. Stradling, J. Phys. C **4**, L38 (1971).
[2] C. Hermann and C. Weisbuch, Phys. Rev. B **15**, 823 (1977).
[3] H. Sigg, J. A. A. J. Perenboom, and P. Wyder, Solid State Commun. **48**, 897 (1983).
[4] W. Zawadzki, P. Pfeffer, and H. Sigg, Solid State Commun. **53**, 777 (1985).
[5] M. A. Hopkins, R. J. Nicholas, P. Pfeffer, W. Zawadzki, D. Gauthier, J. C. Portal, and M. A. DiForte-Poisson, Semicond. Sci. Technol. **2**, 568 (1987).
[6] H. Sigg, J. A. A. J. Perenboom, P. Pfeffer, and W. Zawadzki, Solid State Commun. **61**, 685 (1987).
[7] C. R. Pidgeon and R. N. Brown, Phys. Rev. **146**, 575 (1966).
[8] P. Pfeffer and W. Zawadzki, Phys. Rev. B **41**, 1561 (1990).
[9] P. Pfeffer and W. Zawadzki, Phys. Rev. B **53**, 12 813 (1996).
[10] S. P. Najda, H. Yokoi, S. Takeyama, N. Miura, P. Pfeffer, and W. Zawadzki, Phys. Rev. B **40**, 6189 (1989).
[11] P. Pfeffer and W. Zawadzki, Phys. Rev. B **37**, 2695 (1988).
[12] W. Zawadzki, P. Pfeffer, S. P. Najda, H. Yokoi, S. Takeyama, and N. Miura, Phys. Rev. B **49**, 1705 (1994); P. Pfeffer, W. Zawadzki, S. P. Najda, H. Yokoi, S. Takeyama, and N. Miura, Physica B **201**, 288 (1994).
[13] N. Miura, Physica B **201**, 40 (1994).
[14] N. Miura, H. Nojiri, T. Takamasu, T. Goto, K. Uchida, H. A. Katori, T. Haruyama, and T. Todo, in *Proceedings of the 6th International Conference Megagauss Field Generation and Related Topics*, edited by M. Cowan and R. B. Spielman (Nova Science, Commack, NY, 1994), p. 125.
[15] H. Nojiri, T. Takamasu, T. Todo, K. Uchida, T. Haruyama, T. Goto, H. A. Katori, and N. Miura, Physica B **201**, 579 (1994).
[16] E. O. Kane, J. Phys. Chem. Solids **1**, 249 (1957).
[17] M. H. Weiler, R. L. Aggarwal, and B. Lax, Phys. Rev. B **17**, 3269 (1978).
[18] I. Gorczyca, P. Pfeffer, and W. Zawadzki, Semicond. Sci. Technol. **6**, 963 (1991).
[19] G. Lindemann, R. Lassnig, W. Seidenbusch, and E. Gornik, Phys. Rev. B **28**, 4693 (1983).
[20] W. Zawadzki, C. Chaubet, D. Dur, W. Knap, and K. Raymond, Semicond. Sci. Technol. **9**, 320 (1994).
[21] D. J. Larsen, J. Phys. Chem. Solids **29**, 271 (1968).
[22] W. Zawadzki, X. N. Song, C. L. Littler, and D. G. Seiler, Phys. Rev. B **42**, 5260 (1990).
[23] Y. Yafet, R. W. Keyes, and E. N. Adams, J. Phys. Chem. Solids **1**, 137 (1956).
[24] E. M. Pokatilov and M. M. Rusanov, Fiz. Tverd. Tela (Leningrad) **10**, 3117 (1968) [Sov. Phys. Solid State **10**, 2458 (1968)].
[25] D. R. Leadley, M. S. Daly, R. J. Nicholas, D. K. Maude, J. C. Portal, J. J. Harris, and C. T. Foxon (unpublished).
[26] B. B. Goldberg *et al.* (unpublished).